Parameter Calibration in Dynamic Simulations of Power Cables in Shallow Water to Improve Fatigue Damage Estimation

Charles Spraul, Vincent Arnal, Patrice Cartraud, Christian Berhault

PARAMETER CALIBRATION IN DYNAMIC SIMULATIONS OF POWER CABLES IN SHALLOW WATER TO IMPROVE FATIGUE DAMAGE ESTIMATION

Charles Spraul
École Centrale de Nantes, LHEEA
Nantes, France

Vincent Arnal
École Centrale de Nantes, LHEEA
Nantes, France

Patrice Cartraud
École Centrale de Nantes, GEM
Nantes, France

Christian Berhault
École Centrale de Nantes, LHEEA
Nantes, France

ABSTRACT

The purpose of this work is to use in situ measurements during service to adjust the estimation of the cumulated damage, and achieve an increased accuracy in predicting the remaining life span of the power cable.

Direct monitoring of fatigue damage is not feasible, nor is it possible to completely measure the power cable response along all its length. Measurements can though be obtained concerning environmental conditions and the floater motion, as well as the cable response in a few points. However numerical simulations are still required to compute the state of stress of the cable.

Therefore the intended monitoring methodology aims at calibrating several parameters from the numerical model with respect to available measurements, in order to reduce the uncertainty on these parameters, and thus the uncertainty on the model output. Selection of these parameters must therefore be based on their influence on damage and on their a priori uncertainty. In this respect marine growth influence on cable characteristics is of particular interest.

INTRODUCTION

Dynamic power cables are key components for floating renewable energy farms. They provide the necessary mean to convey energy production from the floating device to the static cable resting on the seabed. Whereas power-grid connection of a bottom-fixed offshore wind turbine benefits from the support structure, the power cable of a floating device needs to be self-supporting and has to accommodate the extreme motions of the floating body due to both dynamic and quasi-static loadings.

Furthermore, repeated loadings at wave frequency impose to qualify dynamic power cables with respect to fatigue. Estimation of the fatigue life is based on the probability of occurrence and on the damage caused by a number of load cases representative of the site. Numerical simulations allow predicting the dynamic response of the cable to those load cases, and the resulting fatigue damage can then be computed. However there is a large uncertainty on this estimation of the fatigue life and most standards require that a safety factor no less than 10 is applied [1, 3].

In the context of renewable energies, this safety factor induces a non-negligible cost as it means larger and heavier cables. On the other hand, reducing arbitrarily this safety factor may lead to failure, and repairs or replacements are also costly as they require the intervention of a specialized ship and an adequate weather window. Accurate prediction of fatigue failure is therefore of particular interest for the planning of such operations at a farm scale.

In order to improve the model accuracy, it is proposed to use available measurements in order to update several parameters of the numerical model.

The calibration method presented in this paper, based on Bayes theory, requires a large number of model evaluations. It is therefore prohibitive to directly use numerical simulations as computational times are too long. Instead a surrogate model needs to be built to replace the direct numerical simulations.

The present paper highlights the limitations of the surrogate model: first in its use to select the parameters to be monitored and the most relevant outputs to be used in the calibration process, then for the calibration process itself.

However, the approach still proves useful to identify the dominant parameters. In the end the overall efficiency of the calibration approach to reduce the uncertainty in damage prediction is evaluated on a test-case configuration.

NOMENCLATURE

m: mass
ρ: water density
V: volume
A: drag area
C_d: drag coefficient
C_a: added-mass coeff.
Hs: significant wave height
Tp: peac period
Gamma: peak coefficient
Dm: mean wave direction
n: wave directional spreading exponent
Uc: current intensity
Dc: current direction
Uw: wind speed
Dw: wind direction
H: water depth
$\vec{a}$: acceleration
$\vec{v}$: velocity
$\vec{a}_f$: fluid acceleration
$\overrightarrow{v_f}$: fluid velocity
X, Y, Z: coordinates
T_hop, T_tdp: tensions at hang of point and touch down point
Cx, Cy: in-plane and out-of-plane curvatures
X_3m: observation of X output at 3m from HOP
X_std: standard deviation of the time signal of X

CONFIGURATION

The configuration studied in this paper is based on the 2MW floating wind turbine (FWT) which is to be installed on the SEM-REV test site as part of the FLOATGEN European project. However, the floater and moorings characteristics used in the study are not definitive, and the power cable configuration presented here was designed purposely for this study, and is not representative of the configuration which will be deployed, in order to avoid confidentiality related conflicts.

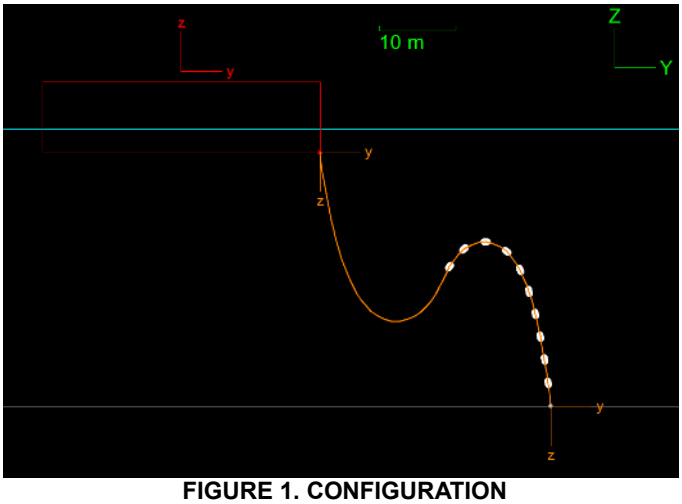

FIGURE 1. CONFIGURATION

The considered FWT has a mass of 5800T and a draft of 7m. The floater, developed by IDEOL, is a square ring 36m wide and 10m high, with a 21x21m moonpool [4]. The wind turbine's nacelle is located 66m above seabed.

The choice of a steep wave configuration, with the power cable connecting vertically to the seabed, was made in order to avoid modelling the cable complex interaction with the seabed [5]. Vertical connection angles at HOP and TDP might not be realistic, however when compared to a more realistic pliant-wave configuration the cable response is very similar away from the cable's ends. The required buoyancy is provided by 10 modules uniformly spaced over the second half of the cable length.

Mean water depth at the SEM-REV test site is 36m. Horizontal distance between the hang-off point (HOP) and the touch-down point (TDP) is set to 30m. Total length of the power cable is 66m.

The power cable plane is orthogonal to the global X axis, which is aligned with the main current direction on site.

Maximum static tension in this nominal configuration is about 3.5kN for a minimum breaking load of roughly 800kN. Bending radius is more critical with a static minimum a little over 3m for a minimum bending radius taken as 1.5m.

TABLE 1. CABLE AND MODULES CHARACTERISTICS

Axial Stiffness	270 kN
Bending Stiffness	3 kN.m²
Torsional Stiffness	30 kN.m²
Mass per unit length	20 kg/m
Diameter	0.1 m
Modules' Mass	50 kg
Modules' Volume	0.125 m³

NUMERICAL MODEL

OrcaFlex time domain simulations

The power cable is modelled in OrcaFlex, an Orcina developed simulation software specialized in dynamic analysis of offshore marine systems [6]. The power cable is discretized in 1m long segments, and its properties are lumped to the nodes, where both external and internal forces and moments are applied. Simulations are performed in time domain to account for all non-linearities.

Axial and torsional stiffness are assumed linear and without coupling. On the other hand, bending behaviour is modelled as hysteretic, using a bilinear model with a dynamic stiffness and a static stiffness (Fig. 2). This model accounts for the frictional behaviour between the power cable internal components. Dynamic stiffness relates to the stick mode, whereas static stiffness relates to the slip mode allowing for relative displacement between internal components. The static stiffness is thus lower than its dynamic counterpart. The power cable starting shape is computed using the static stiffness. During dynamic simulation dynamic stiffness is used except when curvature variations exceed a limit value, in which case static stiffness is used, causing hysteresis and energy dissipation.

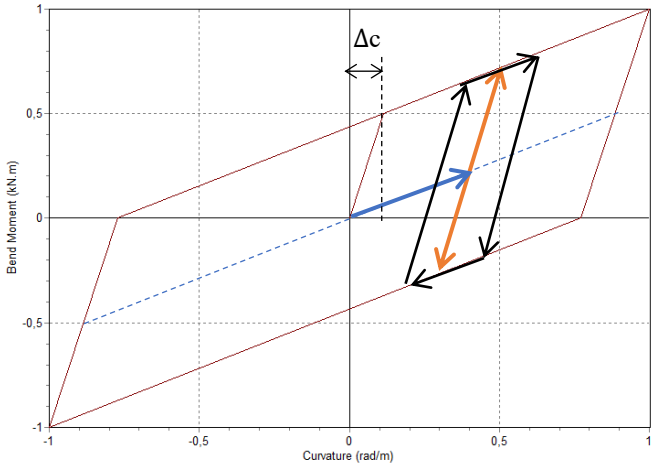

FIGURE 2. BENDING HYSTERESIS

The hydrodynamic loads on the power cable are modelled using Morison's equation (Eq. 1), assuming contribution from both drag and inertia forces.

$$\overrightarrow{F_{Hd}} = \rho V \overrightarrow{a_f} + \rho V C_a \left(\overrightarrow{a_f} - \vec{a}\right) + \frac{1}{2}\rho C_d A \left\|\overrightarrow{v_f} - \vec{v}\right\| \left(\overrightarrow{v_f} - \vec{v}\right) \quad \text{(Eq. 1)}$$

The motion of the FWT is imposed using motion RAO computed externally. Indeed the power cable response has negligible effect on the floater motion. Validity of the floater's motion RAO over the whole range of load cases applied in this study has not been checked, but it appears sufficiently realistic for this study purpose. Details are given below.

The duration of the simulations is set to 2000s in order to obtain good estimations of the means and standard deviations of the observed outputs. Nonetheless, this duration might be insufficient to get a converged estimation of the average damage [1].

Floater motions

The hydrodynamic loads on the FWT's floater are computed using the NEMOH solver (BEM) including 1st order wave load, added-mass and radiation damping [7]. The motion RAO are then computed accounting for hydrostatic and mooring stiffness. Viscous damping is added in heave, roll and pitch to account for the presence of damping plates around the floater. Unsteady aerodynamic loads though are not accounted for. Motion RAO in heave and pitch are given on the figure below for 0° wave incidence.

Low frequency wave and wind loads are not considered in this study, though they might have a significant effect.

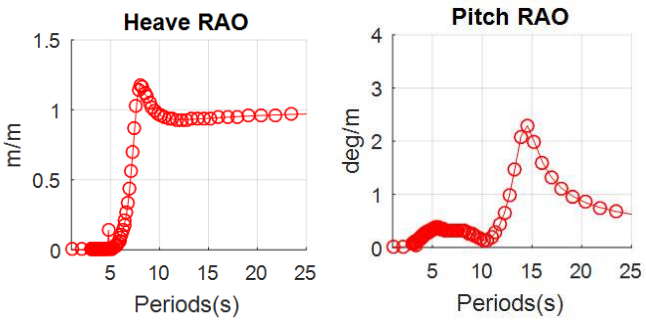

FIGURE 3. MOTION RAO

Floater steady offsets

The FWT steady offsets in surge, sway, roll and pitch are computed externally and imposed as the floater mean position in the OrcaFlex dynamic simulations. These offsets account for the wind and current forces acting on the FWT, as well as the steady wave drift. Hydrostatic and mooring stiffness act as reacting forces.

Environment

Wind is modelled as a constant force acting on the FWT, depending on wind flow average velocity and direction.

Current velocity is set null on the seabed and follows a power law with exponent equals to 7 up to the free surface. The direction of the current is constant.

Irregular waves are modelled using a JONSWAP spectrum with directional spread.

Damage

Local stress within the power cable outer armour layer is computed based on Papaillou formulation [8], accounting for friction with the internal layer. Stress cycles are extracted from the time history using the RainFlow Counting algorithm [9]. Damage is then estimated using DNV SN curve for small diameter umbilical [2] and summed using Palmgren-Miner's rule.

The damage value computed for a given load case represents the proportion of the fatigue life that has been consumed over the duration of the simulation.

In this study damage is evaluated only for the armour outer layer as it is meant to provide the structural strength of the cable, and to protect internal components. It is however not sure that this layer is more critical with respect to fatigue than the conductor cores [10].

Even though damage is observed as an output of the model, the present study focuses on the global response of the power cable. Therefore the influence on damage uncertainty of SN curves parameters and local stress model parameters are not studied though they are likely important.

STOCHASTIC VARIABLES

In this study all parameters are considered as stochastic variables taking their values between 0 and 1. A distinction is though made between environmental parameters and cable or modules parameters. Indeed it is assumed that environmental parameters are monitored and follow known distributions, whereas cable and modules parameters have a fixed but unknown value.

The following tables give the range used for each parameter. For cable and modules parameters these are the a priori uncertainty ranges afflicting the parameters. The objective of the calibration process is to reduce the width of these uncertainty intervals.

TABLE 2. ENVIRONMENTAL PARAMETERS

Hs	0	5	m	Uc	-0.6	0.6	m/s
Tp	2	22	s	Dc	-15°	+15°	
Gamma	1	5		Uw	0	20	m/s
Dm	-45°	0°		Dw	-180°	+180°	
N	5	35		H	33	39	m

TABLE 3. CABLE PARAMETERS

EA	240	300	kN	c_mass	20	50	kg/m
EI_dyn	2	4	kN.m²	c_buoy	-18	-10	kg/m
EI_ratio	0.5	1		c_drag	50	150	kg/m²
Δc	0.1	0.2	1/m	c_add	5	50	kg/m

TABLE 4. MODULES PARAMETERS

m_mass	50	150	kg	m_drag	100	250	kg/m
m_buoy	50	80	kg	m_add	100	300	kg

All stochastic variables are assumed to follow a uniform distribution over their range of variation, and to be independent.

Environment

Waves JONSWAP spectrum is varied using its Hs, Tp and γ parameters. Mean wave direction Dm is also varied as well as the spreading exponent n.

The current on site is mainly due to atmospheric tides. The current speed at free surface level Uc can thus be positive or negative, in which case the actual current direction is Dc + 180°. In the same manner, wind parameters are its speed Uw and direction Dw.

In shallow water tide is assumed to have a significant impact, thus the water depth H is varied between LAT and HAT (lowest and highest astronomic tides).

Power cable structural parameters

Cable axial stiffness EA is varied as well as its bending dynamic stiffness EI_dyn, mainly to investigate the influence of these parameters on the cable response. To further investigate the influence of the hysteretic bending behavior, the ratio between static and dynamic bending stiffness EI_ratio is also taken as a parameter, as well as the limit curvature range Δc which marks the transition between dynamic and static stiffness (Fig. 2).

The uncertainty ranges on these structural parameters could actually be much reduced considering the calibration process only as those parameters can be estimated through mechanical testing. However the purpose here is also to quantify the influence of these parameters at early design stages. This should be considered when looking at the results.

Marine growth dependent power cable parameters

Bio-colonization can affect significantly the cable mass, effective diameter and skin roughness, thus changing the hydrodynamic loads on the cable. Locally the marine growth can be described using its thickness, density and roughness as parameters [11]. However the choice is made in this study to rather employ its effect on the cable mass, hydrostatic and hydrodynamic characteristics as parameters. Thus the cable mass, net buoyancy, drag and added-mass are used to model the marine growth effect on the cable. Those parameters are highlighted in bold in the dynamic equilibrium equation of a cable node given below (Eq. 2 and 3).

$$\boldsymbol{m}\,\vec{a} = (\boldsymbol{m} - \boldsymbol{\rho V})\,\vec{g} + \rho V\,\overrightarrow{a_f} + \boldsymbol{\rho V C_a}\left(\overrightarrow{a_f} - \vec{a}\right) + \frac{\mathbf{1}}{\mathbf{2}}\boldsymbol{\rho C_d A}\left\|\overrightarrow{v_f} - \vec{v}\right\|\left(\overrightarrow{v_f} - \vec{v}\right) + \overrightarrow{T_1} + \overrightarrow{T_2} + \overrightarrow{\text{Shear}} \quad \text{(Eq. 2)}$$

$$\boldsymbol{mass}\,\vec{a} = \boldsymbol{buoy}\,\vec{g} + \rho V\,\overrightarrow{a_f} + \boldsymbol{add}\left(\overrightarrow{a_f} - \vec{a}\right) + \boldsymbol{drag}\left\|\overrightarrow{v_f} - \vec{v}\right\|\left(\overrightarrow{v_f} - \vec{v}\right) + \overrightarrow{T_1} + \overrightarrow{T_2} + \overrightarrow{\text{Shear}} \quad \text{(Eq. 3)}$$

For this study it is considered that the marine growth thickness can vary between 0 and 5 cm on the cable, and between 0 and 10 cm on the modules which offer a wider surface. A fixed density of 1300 kg/m^3 is used to determine the mass and net buoyancy parameters as a function of marine growth thickness. For drag and added-mass parameters, the effect of roughness variations is also included, considering Cd between 0.8 and 1.2 and Ca between 0.7 and 1.3.

It is assumed here that the marine growth repartition is uniform over the cable length. However marine growth effect on the buoyancy modules is modelled with a distinct set of parameters, which allow, to some extent, studying the effect of marine growth repartition.

SURROGATE MODEL

The surrogate model approximates the model outputs with the advantage of a much reduced evaluation time. This approach is extensively used in reliability analysis when a large number of model evaluations are required and when model evaluations are time consuming [12]. Construction of a surrogate model though implies disposing of a training data set, consisting of paired inputs and outputs obtained through model evaluations.

Validity of the surrogate model is thus restricted to the domain covered by the experiment design of the inputs in the training data set.

The surrogate model used in this study is the polynomial chaos algorithm implemented in OpenTURNS [13]. A cleaning strategy is used to keep at most 50 terms based on their significance. Maximum polynomial degree is 3.

The experiment design employed in this study is Monte Carlo sampling of the 22 stochastic variables described above over their whole respective range of variation, with the exception that samples that do not verify (Eq. 4) are rejected. This is done to avoid simulating unrealistic sea states; it however introduces correlation between these two variables.

$$2\,Hs < Tp - 2 \qquad \text{(Eq. 4)}$$

The surrogate model is built from a data base consisting of 4000 load cases with inputs samples drawn according to the experiment design described above. For each load case, time signals of several outputs are returned by the numerical simulation. For each one, the mean value and the standard deviation are recorded. The observed outputs are: tensions at HOP and TDP (T_hop, T_tdp), and curvatures (Cx: in-plane and Cy: out-of-plane) and spatial coordinates (X, Y, Z) at 3m, 24m, 36m, 42m and 54m from HOP. Furthermore damage is computed every 3m from 3m to 60m. For each load case the maximum damage is the maximum damage observed over the power cable length.

For each recorded output a surrogate model can be constructed. The efficiency of the surrogate model is though dependent on the on the complexity of the relation between the stochastic variables inputs and the observed output. Indeed, nonlinearities or strong effects of the interactions between the input variables are more difficult to capture properly, and usually require increasing the maximum polynomial degree, which is impractical with too many input variables.

The efficiency of the surrogate model is evaluated for each output by computing the normalized root mean square error (NRMSE). Figures 4, 5 and 6 compare the surrogate model predictions with the simulations outputs for the HOP tension mean value, the standard deviation of the in-plane curvature at 3m from HOP, and the maximum damage respectively.

The surrogate model error is large on damage prediction and on curvatures. Good predictions can though be obtained for tension and position outputs.

To reduce the surrogate model error it is possible to increase the number of points in the learning data set, or to increase the maximum polynomial degree of the polynomial chaos expansion. However both solutions are time consuming. For the purpose of the sensitivity study presented in the following, it is assumed that the surrogate model precision is sufficient to capture the dominant effects. Caution should though be observed when considering the effect of less dominant parameters.

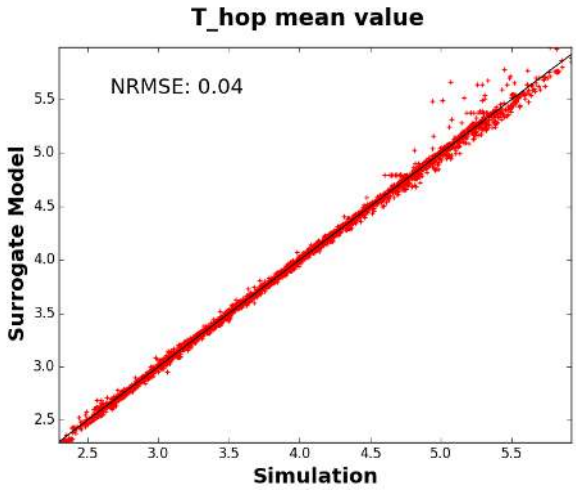

FIGURE 4. SURROGATE MODEL PREDICTION OF HOP TENSION MEAN VALUE [KN]

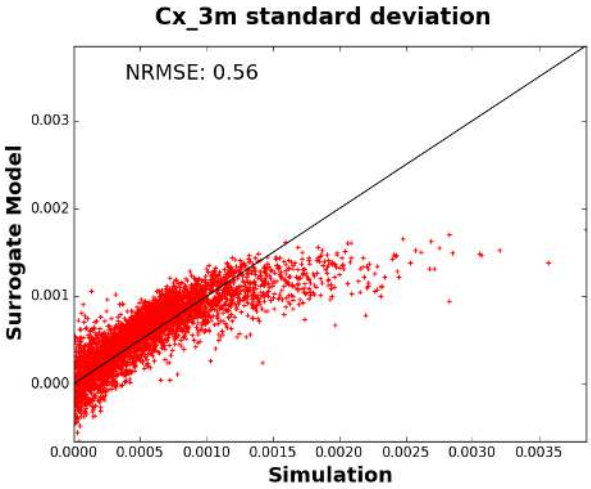

FIGURE 5. SURROGATE MODEL PREDICTION OF IN-PLANE CURVATURE STANDARD DEVIATION AT 3M FROM HOP [1/M]

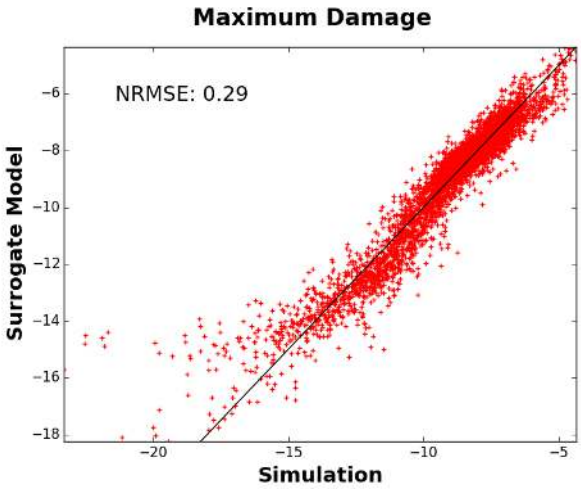

FIGURE 6. SURROGATE MODEL PREDICTION OF MAXIMUM DAMAGE [-] (LOG SCALE)

CHOICE OF PARAMETERS FOR CALIBRATION

In order to reduce the uncertainty on the estimation of the power cable damage, influential parameters have to be calibrated. The most influential parameters are chosen based on a sensitivity analysis.

The sensitivity analysis performed in this study is based on the method ANOVA (ANalysis Of VAriance) [14]. For each parameter, the total order Sobol index is computed to measure the parameter influence on the output. The total order Sobol index gives the proportion of output variance that is related to the parameter, including the effect of interactions with the other parameters.

Computation of the Sobol indices requires a specific experiment design, and a large number of model evaluations. Direct numerical simulation is therefore impractical and the surrogate model is used instead.

The observed output is the maximum damage over the cable length. Results are presented on figures 7 and 8. As expected, environmental parameters and especially waves' are dominant.

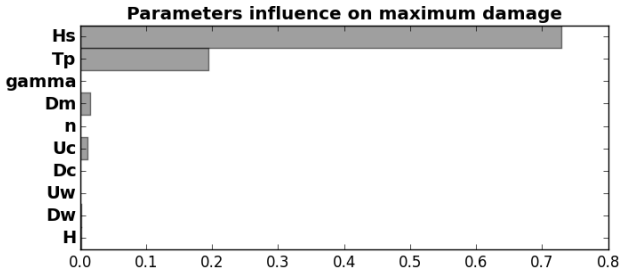

FIGURE 7. TOTAL ORDER SOBOL INDICES OF ENVIRONMENTAL PARAMETERS WITH RESPECT TO MAXIMUM DAMAGE

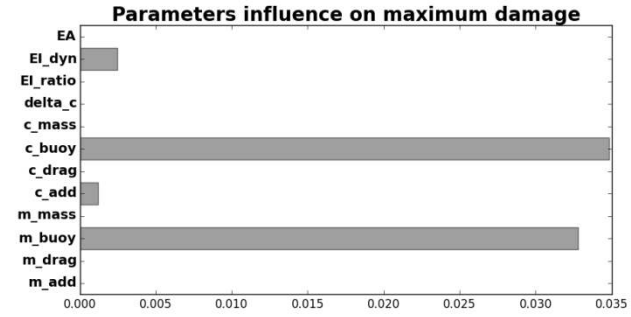

FIGURE 8. TOTAL ORDER SOBOL INDICES OF THE CABLE PARAMETERS WITH RESPECT TO MAXIMUM DAMAGE

Considering the cable parameters, the most influential parameters, which are selected for calibration, are the net buoyancies of the cable section and of the modules (c_buoy and m_buoy respectively).

Other parameters appear to have negligible influence. Nonetheless, the EI_dyn and c_add parameters are also kept for calibration. Although as their Sobol indices are two orders of magnitude lower than that of Hs and Tp, and given the surrogate model error, it is not sure whether these parameters are actually more influential than others or not.

CHOICE OF MOST RELEVANT OUTPUTS

The number of available measurements on the cable response is limited by the sensors which can be installed on (or in) the power cable. Therefore, even without considering the practical feasibility of measuring a given output, it is important to limit the number of outputs that are used in the calibration process.

The choice of a relevant set of outputs can be based on their sensitivity to the calibrated parameters. Sobol indices are thus computed for the different outputs that were recorded in the data base. Figures 9, 10, 11 and 12 present the results for the 4 selected parameters. For each parameter, only the outputs with the largest indices are represented.

The different outputs that are studied are the tensions, curvatures and positions at different locations along the cable. For each output, both the mean value and standard deviation are considered. The objective is to find out which measurements should be taken at which location to efficiently calibrate the outputs.

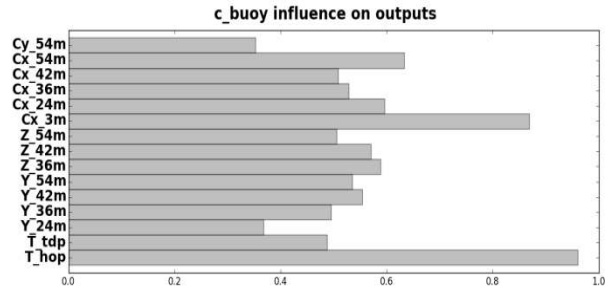

FIGURE 9. MEASURE OF THE CABLE SECTION NET BUOYANCY INFLUENCE ON A SELECTION OF OUTPUTS

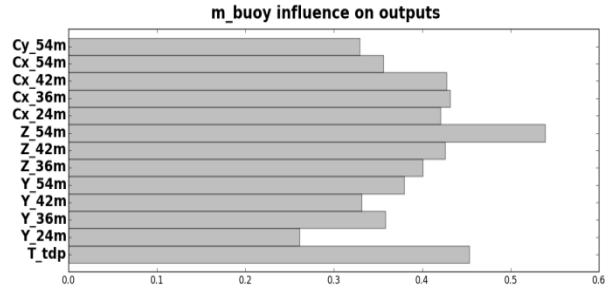

FIGURE 10. MEASURE OF THE MODULES NET BUOYANCY INFLUENCE ON A SELECTION OF OUTPUTS

C_buoy and M_buoy have a strong influence on several outputs and should thus be easily calibrated.

In particular, the mean tension values at HOP and TDP can be used to calibrate these two parameters. But actually most of the outputs related to the in-plane mean response of the cable could be used effectively.

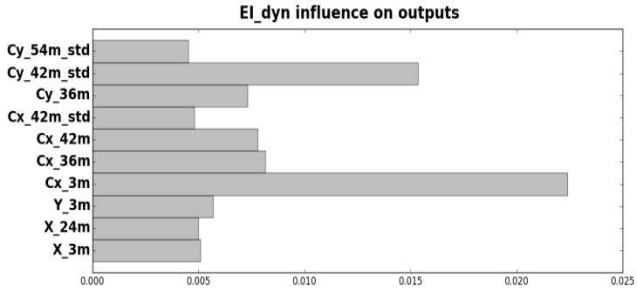

FIGURE 11. MEASURE OF THE DYNAMIC BENDING STIFFNESS INFLUENCE ON A SELECTION OF OUTPUTS

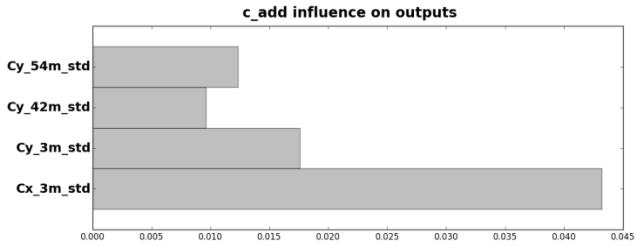

FIGURE 12. MEASURE OF THE CABLE SECTION ADDED MASS INFLUENCE ON A SELECTION OF OUTPUTS

EI_dyn and C_add on the other hand have weak influences on all the outputs. Several outputs are thus picked for their calibration: Cx_3m, Cx_3m_std, Cy_3m_std, Cy_42m_std, and Cy_54m_std.

As the indices are very low, it is difficult to draw any conclusions. However both parameters rather affect curvatures standard deviations, which are strongly related to damage, and mainly near the HOP and in the modules area.

The calibration is performed using the surrogate model. The error of the surrogate model on the selected outputs should thus be checked. NRMSE values are given in following table. Except for the tensions, the surrogate model errors are large.

TABLE 5. NRMSE OF THE SURROGATE MODEL ON SELECTED OUTPUTS

T_hop	0.04	Cy_3m_std	0.30
T_tdp	0.02	Cy_42m_std	0.43
Cx_3m	0.22	Cy_54m_std	0.28
Cx_3m_std	0.41		

BAYESIAN CALIBRATION

Bayesian calibration is a probabilistic method to estimate best-fitting values of the model's parameters from a set of observations. The advantage over least square calibration is that this method returns the probabilistic distributions of the calibrated parameters, accounting for the remaining uncertainties. However the calibration requires a large number of model evaluations, as the calibrated distributions are determined through Markov Chain Monte Carlo simulations (MCMC). The surrogate model is employed for that purpose.

The Bayesian calibration process used in this study is the Metropolis Hasting algorithm implemented in OpenTURNS [13].

In order to evaluate the efficiency of the calibration method, a fixed value is attributed to each of the cable and modules' parameters. Then 40 load cases are simulated for random environmental conditions and the calibration method is applied to find the fixed values of the parameters which have to be calibrated.

Simulation outputs as well as environmental inputs, for each of the 40 load cases, constitute the observations used in the calibration process. The simulation outputs are the 7 outputs selected in the previous section.

Prior to the calibration a uniform distribution is assumed for the calibrated parameters. In this study, all cable parameters that are not calibrated are assumed to be known. A next step would be to introduce an error on these parameters.

The calibration process then uses MCMC to perform a random sampling that converges toward the post calibration distribution. The surrogate model is employed to evaluate the likelihood function of the parameters according to the observations.

At the end of the calibration process, independent normal distributions are assumed for the calibrated parameters and the distributions' parameters are set to fit the sampled distributions. Figure 13 present for each parameter its distribution before and after the calibration, as well as its expected value. Table 7 summarizes the parameters values and uncertainties resulting from the calibration.

TABLE 7. CALIBRATION RESULTS

	EI_dyn	*C_buoy*	*C_add*	*M_buoy*
Fixed value	0.650	0.375	0.556	0.333
Calibration mean value	0.634	0.375	0.322	0.333
Remaining uncertainty	0.124	0.004	0.082	0.004

The calibration process has proved efficient for C_buoy and M_buoy. That was indeed expected as those parameters have a large influence on the two outputs on which the surrogate model error is low: T_hop and T_tdp.

The results on C_add on the other hand show the limitation of the calibration method when there is a large error between the surrogate model and the observations.

Concerning EI_dyn though, the calibration results appear to be quite good since there is also a large error on the outputs that were selected for its calibration.

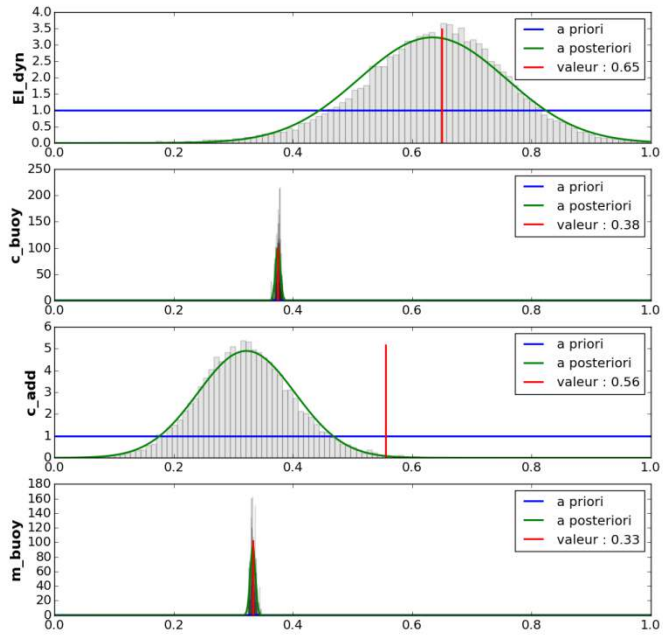

FIGURE 13. PARAMETERS DISTRIBUTIONS AFTER CALIBRATION

EFFECT OF CALIBRATION ON DAMAGE UNCERTAINTY

In this section d denotes the damage as a function of environmental parameters and of cable parameters, and D the statistical expectation of the damage over all environmental conditions for a given set of cable parameters values.

The uncertainty on the damage prediction σ_D is taken as the standard deviation of D when only cable parameters are varied. In practice the variance $V_{\theta_{cable}}(D)$ can be considered as a first order Sobol index (Eq. 7) and estimated as such using Jansen estimator [15].

$$D(\theta_{cable}) = E_{\theta_{envir}}(d(\theta_{envir}, \theta_{cable}) \mid \theta_{cable}) \quad \text{(Eq. 5)}$$

$$\sigma_D = \sqrt{V_{\theta_{cable}}(D)} \quad \text{(Eq. 6)}$$

$$V_{\theta_{cable}}(D) = V_{\theta_{cable}}\left(E_{\theta_{envir}}(d \mid \theta_{cable})\right) \quad \text{(Eq. 7)}$$

Using the calibration case of the previous section, the expected value of D and its uncertainty can both be computed considering either the pre-calibration distributions or the post-calibration distributions. It is therefore possible to quantify the effect of the calibration. The considered damage value here is the maximum damage value, which is evaluated using the surrogate model.

The uncertainties values given in table 8 are only related to the cable parameters uncertainties and do not consider the uncertainty due to the use of the surrogate model. It can be observed that the uncertainty due to the cable parameters has been reduced by an order of magnitude thanks to the calibration. It is however still of the same order of magnitude as the expected value. Calibration of the net buoyancies of both cable and modules thus appears to be useful. However a large uncertainty remains associated with the cable parameters, thus implying further reduction of those parameters uncertainty ranges might be useful.

Caution must though be observed as those conclusions are drawn from a single test case. In addition the uncertainty ranges on the cable parameters are likely quite large and their distributions were assumed independent, while dominant parameters are all strongly related to marine growth thickness. A more realistic probabilistic modelling should thus lead to a lower uncertainty on damage.

TABLE 8. EFFECT OF THE CALIBRATION ON DAMAGE UNCERTAINTY

	Expected value of D	σ_D
Prior distribution	3.07 e-7	3.16 e-6
Posterior distribution	7.12 e-8	2.92 e-7
Fixed values	8.01 e-8	-

CONCLUSIONS

A test-case configuration was defined based on the FLOATGEN FWT to be installed on the SEMREV test site.

A sensitivity analysis was conducted using the ANOVA method to determine the most influential cable parameters on damage, as well as to find a relevant set of outputs for the calibration of those influential parameters.

For that purpose a surrogate model was built, using a polynomial chaos expansion. The error measured between the surrogate model and the numerical simulation was however large for several outputs, including the damage.

Marine growth effect on the cable was modelled using its effect on the cable mass, net buoyancy, and hydrodynamic drag and added mass.

Most influential cable parameters were found to be the net buoyancies of the cable and of the modules which are both strongly dependent on the marine growth thickness and density. These two parameters can be efficiently calibrated using only the mean values of tensions at HOP and TDP which are predicted accurately by the surrogate model.

By calibrating these two parameters on a test case, the uncertainty on damage due to cable parameters was reduced by an order of magnitude.

Other cable parameters influence on damage appeared to be negligible. However, given the dominant role of wave Hs and Tp parameters, it seemed difficult to evaluate with precision the influence of the less influential parameters. Especially since the surrogate model error was large.

A crude estimation of the damage uncertainty caused by those parameters in the last section seems to indicate that their impact on damage might actually not be negligible.

In further work to quantify the influence of these parameters on the dynamic response, it appears necessary to focus on a limited number of load cases in order to remove

environmental parameters influence. Cable and modules net buoyancies could also be fixed as they can easily be calibrated independently from other cable parameters.

ACKNOWLEDGMENTS

The authors would like to thanks the European project FLOATGEN as well as the French region Pays de la Loire for their financial support.

REFERENCES

[1] DNV RP-F204. Riser Fatigue, (2005).

[2] DNV RP-C203. Fatigue Design of Offshore Steel Structures, (2010).

[3] DNV RP-F401. Electrical Power Cables in Subsea Applications, (2012).

[4] Guignier, L., Courbois, A., Mariani, R., Choisnet, T., Multibody Modelling of Floating Offshore Wind Turbine Foundation for Global Loads Analysis, ISOPE (2016).

[5] Shiri, H., Randolph, M., The Influence of Seabed Response on Fatigue Performance of Steel Catenary Risers in Touchdown Zone, OMAE (2010).

[6] https://www.orcina.com/SoftwareProducts/OrcaFlex

[7] Babarit, A., Delhommeau, G., Theoretical and numerical aspects of the open source BEM solver NEMOH, EWTEC (2015).

[8] Papailiou, K.O., On the Bending Stiffness of Transmission Line Conductor, IEEE Transactions on Power Delivery (1997).

[9] Amzallag, C., Gerey, J.P., Robert, J.P., Bahuaudl, J., Standardization of the rainflow counting method for fatigue analysis, Int. Journal of Fatigue (1994).

[10] Nasution, F.P., Sævik, S., Gjøsteen, J.K.Ø., Finite element analysis of the fatigue strength of copper power conductors exposed to tension and bending loads, Int. Journal of Fatigue, (2014).

[11] Ameryoun, H., Schoefs, F., Probabilistic Modeling of Roughness Effects Caused by Bio-Colonization on Hydrodynamic Coefficients: A Sensitivity Study for Jacket-Platforms in Gulf of Guinea, OMAE (2013).

[12] Quéau, L.M., Kimiaei, M., Randolph, M.F., Approximation of the maximum dynamic stress range in steel catenary risers using artificial neural networks, Engineering Structures (2015).

[13] Baudin, M., Lebrun, R., Loss, B., Popelin, A. L., Open TURNS: An industrial software for uncertainty quantification in simulation, Handbook of Uncertainty Quantification (2015).

[14] Sobol, I. M., Sensitivity analysis for non-linear mathematical model, Math. Modelling Comput. Exp., 1993, 1, 407-414.

[15] Jansen, M.J.W. *Analysis of variance designs for model output*, Computer Physics Communication, 1999, 117, 35-43.